Buoyancy effects on the 3D MHD stagnation-point flow of a Newtonian fluid

A. Borrelli[a], G. Giantesio[b], M.C. Patria[a], A.V. Roşca[d], N.C. Roşca[c], I. Pop[c]

[a]*Dipartimento di Matematica e Informatica, Università di Ferrara, via Machiavelli 35, 44121 Ferrara, Italy*
[b]*Dipartimento di Matematica e Fisica, Università Cattolica del Sacro Cuore, via Musei 41, 25121 Brescia, Italy*
[c]*Department of Mathematics, Faculty of Mathematics and Computer Science, Babeş-Bolyai University, str Mihail Kogalniceanu 1, Cluj-Napoca, Romania*
[d]*Department of Statistics-Forecasts-Mathematics, Faculty of Economics and Business Administration, Babeş-Bolyai University, str Mihail Kogalniceanu 1, Cluj-Napoca, Romania*

Abstract

This work examines the steady three-dimensional stagnation-point flow of an electrically conducting Newtonian fluid in the presence of a uniform external magnetic field $\mathbf{H}_0$ under the Oberbeck-Boussinesq approximation. We neglect the induced magnetic field and examine the three possible directions of $\mathbf{H}_0$ which coincide with the directions of the axes.

In all cases it is shown that the governing nonlinear partial differential equations admit similarity solutions. We find that the flow has to satisfy an ordinary differential problem whose solution depends on the Hartmann number M, the buoyancy parameter λ and the Prandtl number Pr.

The skin-friction components along the axes are computed and the stagnation-point is classified. The numerical integration shows the existence of dual solutions and the occurrence of the reverse flow for some values of the parameters.

Keywords: Newtonian fluids; MHD fully developed flow; Boussinesq approximation; three-dimensional stagnation-point flow.

1. Introduction

The case of a steady magnetohydrodynamic (MHD) stagnation-point flow of an electrically conducting fluid has several applications because it appears in a very common situation: a jet of fluid impinges on a rigid body in the presence of an electromagnetic field.

The study of the MHD stagnation-point flow of an electrically conducting fluid in the presence of an external magnetic field was considered by several authors

[1, 2, 3, 4, 5, 6, 7, 8, 9, 10, 11].

Mixed convection flows, or combined forced and free convection flows, play an important role, for example, in atmospheric boundary-layer flows, heat exchangers, solar collectors, nuclear reactors and in electronic equipment. Such processes occur when the effects of buoyancy forces in forced convection or the effects of forced flow in free convection become significant. Over the previous decades many analyses of mixed convection flow of a viscous and incompressible fluid over a vertical surface have been performed ([12, 13, 14, 15, 16]).

This present paper aims to study the problem of a MHD mixed convection boundary layer flow toward a stagnation point on a vertical flat plate in the presence of a magnetic field where the effects of the induced magnetic field are neglected and under the Boussinesq approximation. The governing partial differential equations are reduced to nonlinear ordinary differential equations that are then solved numerically. The flow depends heavily on the Hartmann number M, the Prandtl number Pr, and the buoyancy parameter λ.

Some numerical examples and pictures are given in order to illustrate the effects due to the magnetic field on the behaviour of the solution. The numerical results are obtained by using the MATLAB routine bvp4c, which is described in [17] and [18]. The obtained results are in good agreement to the one reported in [19, 20, 21, 22].

From the numerical integration, it appears that dual solutions exist for some values of the parameters, as it is reported in literature for similar problems ([23, 24, 20, 25, 26, 27, 28, 29, 30, 31]).

Moreover, we classify the stagnation-point as nodal or saddle point and as attachment or separation point and we discuss the occurence of the reverse flow ([21, 22, 2, 3]).

The paper is organized in this way:

In Section 2, we study the three-dimensional stagnation-point flow of an inviscid fluid in the presence of a uniform external electromagnetic field and of the gravity forces. Following [2] it is easy to prove Theorem 2 which states that, if we impress an external magnetic field $\mathbf{H}_0$, and we neglect the induced magnetic field, then the steady three-dimensional MHD stagnation-point flow of such a fluid is possible for any value of $c > -1$ (the parameter c is a measure of the three-dimensionality of the motion) if $\mathbf{H}_0$ has the direction parallel to one of the axes. Further if $c = 1$, or $c = -\frac{1}{2}$, we prove that the magnetic field can be parallel also to the plane Ox_1x_3, or Ox_2x_3 respectively.

In Section 3, we determine the nonlinear ODE problems for a Newtonian fluid under the Boussinesq approximation corresponding to the cases treated in Theorem 2. Moreover, in proposition 6 we prove that if $c = 1$ or $c = -\frac{1}{2}$, then the three-dimensional MHD stagnation point flow is not possible when $\mathbf{H}_0$ is parallel to the plane Ox_1x_3 or Ox_2x_3, unlike what occurs to the inviscid fluid. We then illustrate the reverse flow pheonomenon and we discuss the classification of the stagnation point.

Section 4 studies the most interesting physical situation when the external magnetic field is orthogonal to the wall. The numerical profiles of the solution are described. We also furnish several tables in order to classify the stagnation-point
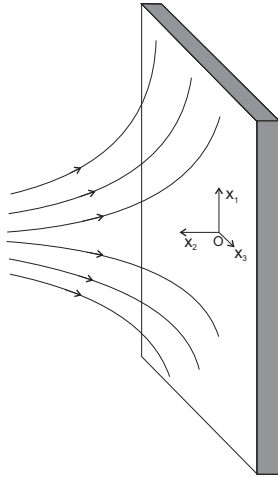
2

Figure 1: Physical model and the coordinate system.

and to point out the occurrence of the reverse flow. From numerical results we have that the external magnetic field tends to prevent the reverse flow while the buoyancy forces tend to favor it. Moreover we show that dual solutions may arise for suitable values of λ and c.

The conclusions are drawn in Section 5.

2. The flow of an inviscid fluid

Consider the steady three-dimensional MHD flow of an electrically conducting homogeneous incompressible inviscid fluid near a stagnation point filling the half-space $\mathcal{S}$, given by

$$\mathcal{S} = \{(x_1, x_2, x_3) \in \mathbb{R}^3 : (x_1, x_3) \in \mathbb{R}^2, x_2 > 0\}. \tag{1}$$

The boundary of $\mathcal{S}$, i.e. $x_2 = 0$, is a rigid, fixed, non-electrically conducting wall.

As it is well known in the three-dimensional stagnation-point flow the velocity field is given by

$$v_1 = ax_1, \quad v_2 = -a(1+c)x_2, \quad v_3 = acx_3, \quad (x_1, x_2, x_3) \in \mathcal{S}, \tag{2}$$

where a, b are constants.

We suppose $a > 0$, $c \neq 0$ (in order to have a three-dimensional motion) and $c > -1$. We exclude the case $c \leq -1$ because we impose the condition $v_2 < 0$, so that the fluid moves towards the wall $x_2 = 0$.

We further suppose that the plane Ox_1x_3 is vertical with Ox_1 vertical upward.

Remark 1. If $c = 1$, then the velocity is axial symmetric with respect to x_2 axis:

$$v_1 = ax_1, \quad v_2 = -2ax_2, \quad v_3 = ax_3.$$

The equations governing such a flow in the presence of the gravity forces are:

$$\rho_0 \mathbf{v} \cdot \nabla \mathbf{v} = -\nabla p^* + \mu_e (\nabla \times \mathbf{H}) \times \mathbf{H} + \rho_0 \mathbf{g}_0,$$

$$\nabla \cdot \mathbf{v} = 0,$$

$$\nabla \times \mathbf{H} = \sigma_e (\mathbf{E} + \mu_e \mathbf{v} \times \mathbf{H}),$$

$$\nabla \times \mathbf{E} = \mathbf{0}, \quad \nabla \cdot \mathbf{E} = 0, \quad \nabla \cdot \mathbf{H} = 0, \qquad \text{in } \mathcal{S} \qquad (3)$$

where $\mathbf{v}$ is the velocity field, p^* is the pressure, $\mathbf{E}$ and $\mathbf{H}$ are the electric and magnetic fields, respectively, ρ_0 is the mass density (constant > 0), μ_e is the magnetic permeability, σ_e is the electrical conductivity ($\mu_e, \sigma_e = $ constants > 0), $\mathbf{g}_0$ is the gravity acceleration.
We suppose that a uniform external magnetic field $\mathbf{H}_0$ is impressed and that the electric field is absent. As it is customary in the literature, we assume that the magnetic Reynolds number is very small, so that the induced magnetic field is negligible in comparison with the imposed field. Then

$$(\nabla \times \mathbf{H}) \times \mathbf{H} \simeq \sigma_e \mu_e (\mathbf{v} \times \mathbf{H}_0) \times \mathbf{H}_0. \qquad (4)$$

In the sequel we will use the modified pressure p given by the difference between the pressure and the hydrostatic pressure, i.e.

$$p = p^* + \rho_0 g_0 x_1.$$

As in [2] one can prove the following:

Theorem 2. Let a homogeneous, incompressible, electrically conducting inviscid fluid occupy the half-space $\mathcal{S}$. If we impress an external magnetic field $\mathbf{H}_0$, and we neglect the induced magnetic field, then the steady three-dimensional MHD stagnation-point flow of such a fluid is possible for all $c > -1$ if, and only if, $\mathbf{H}_0$ is parallel to one of the axes.

If $\mathbf{B}_0 \equiv \mu_e \mathbf{H}_0 = B_0 \mathbf{e}_1$ we deduce

$$p = -\rho_0 \frac{v^2(x_1, x_2, x_3)}{2} + \frac{a}{2} \sigma_e B_0^2 [(1 + c)x_2^2 - cx_3^2] + p_0; \qquad (5)$$

if $\mathbf{B}_0 \equiv \mu_e \mathbf{H}_0 = B_0 \mathbf{e}_2$ we deduce

$$p = -\rho_0 \frac{v^2(x_1, x_2, x_3)}{2} - \frac{a}{2} \sigma_e B_0^2 (x_1^2 + cx_3^2) + p_0; \qquad (6)$$

if $\mathbf{B}_0 \equiv \mu_e \mathbf{H}_0 = B_0 \mathbf{e}_3$ we deduce

$$p = -\rho_0 \frac{v^2(x_1, x_2, x_3)}{2} - \frac{a}{2} \sigma_e B_0^2 [x_1^2 - (1 + c)x_2^2] + p_0. \qquad (7)$$

4

Remark 3. *The results obtained in Theorem 2 hold for any $c > -1$. We remark that if $c = 1$, it is possible to consider also the magnetic field parallel to the plane Ox_1x_3 as outlined in [2]. In this case*

$$p = -\rho \frac{v^2(x_1, x_2, x_3)}{2} + a\sigma_e(B_{01}^2 + B_{03}^2)x_2^2 - \frac{a}{2}\sigma_e(B_{03}x_1 - B_{01}x_3)^2 + p_0.$$

Moreover, if $c = -\dfrac{1}{2}$ it is possible to consider the magnetic field parallel to the plane Ox_2x_3, as in [2]. The corresponding modified pressure is

$$p = -\rho \frac{v^2(x_1, x_2, x_3)}{2} - \frac{a}{2}\sigma_e(B_{02}^2 + B_{03}^2)x_1^2 + \frac{a}{4}\sigma_e(B_{03}x_2 - B_{02}x_3)^2 + p_0.$$

Remark 4. *We notice that, from (5), (6), (7), the modified pressure along the wall $x_2 = 0$ takes its maximum in the stagnation-point.*

Remark 5. *In order to study the three-dimensional stagnation-point flow for other fluids, it is convenient to consider a more general flow. More precisely, we suppose the fluid impinging on the flat plane $x_2 = C$ and*

$$v_1 = ax_1, \quad v_2 = -a(1+c)(x_2 - C), \quad v_3 = acx_3, \quad (x_1, x_3) \in \mathbb{R}^2, \quad x_2 \geq C, \ (8)$$

with C some constant.
In this way, the stagnation point is not the origin but the point $(0, C, 0)$.
As it is easy to verify, in the cases of Theorem 2 and Remark 3 the expression of p must be modified by replacing x_2 with $x_2 - C$.

3. Newtonian Fluids: analysis of the flow

If the fluid is Newtonian we apply the Boussinesq approximation and suppose that the plane Ox_1x_3 is vertical (Ox_1 vertical upward), the equations for such a fluid are

$$\mathbf{v} \cdot \nabla \mathbf{v} = -\frac{1}{\rho_0}\nabla p + \nu \triangle \mathbf{v} + \frac{\mu_e}{\rho_0}(\nabla \times \mathbf{H}) \times \mathbf{H} - \alpha_T(T - T_0)\mathbf{g}_0,$$

$$\nabla \cdot \mathbf{v} = 0,$$

$$\nabla T \cdot \mathbf{v} = \beta \triangle T,$$

$$\nabla \times \mathbf{H} = \sigma_e(\mathbf{E} + \mu_e \mathbf{v} \times \mathbf{H}),$$

$$\nabla \times \mathbf{E} = \mathbf{0}, \quad \nabla \cdot \mathbf{E} = 0, \quad \nabla \cdot \mathbf{H} = 0, \qquad \text{in } \mathcal{S} \qquad (9)$$

where T_0 is the reference temperature, ν is the kinematic viscosity relative to ρ_0 which is the constant mass density corresponding to T_0, β is the thermal diffusivity, α_T is the thermal expansion coefficient.
It is assumed that the temperature around $\mathcal{S}$ is T_0.
As far as the boundary conditions for $\mathbf{v}$ and T are concerned, we prescribe:

$$\mathbf{v}|_{x_2=0} = \mathbf{0}, \quad T|_{x_2=0} = Dx_1 + T_0 \equiv T_w(x_1) \qquad (10)$$

where D is constant.

If the constant D is positive (negative), then the wall $x_2 = 0$ is hotter (colder) than the environment at $x_1 > 0$, while it is colder (hotter) than the environment at $x_1 < 0$.

We search $\mathbf{v}$ and T in the following form:

$$v_1 = ax_1 f'(x_2), \quad v_2 = -a[f(x_2) + cg(x_2)], \quad v_3 = acx_3 g'(x_2),$$
$$T = (T_w(x_1) - T_0)\theta(x_2) + T_0, \quad \forall (x_1, x_2, x_3) \in \mathcal{S}, \tag{11}$$

where f, g, θ are sufficiently regular unknown functions.

The conditions (10) supply

$$f(0) = 0, \quad f'(0) = 0, \quad g(0) = 0, \quad g'(0) = 0, \ \theta(0) = 1. \tag{12}$$

Moreover, as is customary when studying the stagnation-point flow for viscous fluids, we assume that at infinity, the flow approaches the flow of an inviscid fluid at the uniform temperature T_0, whose velocity is given by (8).

Therefore, to (12) we also must append the following conditions

$$\lim_{x_2 \to +\infty} f'(x_2) = 1, \quad \lim_{x_2 \to +\infty} g'(x_2) = 1, \ \lim_{x_2 \to +\infty} \theta(x_2) = 0. \tag{13}$$

The constant C in (8) is related to the behavior of f and g at infinity. Actually, if

$$\lim_{x_2 \to +\infty} [f(x_2) - x_2] = -A, \quad \lim_{x_2 \to +\infty} [g(x_2) - x_2] = -B \tag{14}$$

with A, B some constants, then

$$\lim_{x_2 \to +\infty} [f(x_2) + cg(x_2) - (1+c)x_2] = -(1+c)C, \tag{15}$$

where

$$C = \frac{A + cB}{1 + c}.$$

The constants A, B, C are not assigned a priori, but their values can be found by solving the problem.

In order to study the influence of a uniform external electromagnetic field in the absence of an electric field, we continue to use approximation (4), where $\mathbf{v}$ is given by (11). As a result of the Theorem 2, $\forall c > -1$, we have to consider three different cases.

In the sequel, we furnish some calculations only in the case when the external magnetic field is orthogonal to the wall, because this situation is more interesting from a physical point of view. Therefore we begin with

$$\mathbf{H}_0 = H_0 \mathbf{e}_2,$$

so that

$$(\nabla \times \mathbf{H}) \times \mathbf{H} \simeq -\sigma_e \mu_e a H_0^2 (x_1 f' \mathbf{e}_1 + cx_3 g' \mathbf{e}_3). \tag{16}$$

6

We substitute (11), and (16) in $(9)_1$ to obtain

$$ax_1 \left[\nu f''' + af''(f + cg) - af'^2 - \frac{\sigma_e a}{\rho_0} B_0^2 f' + \frac{\alpha_T g_0 D}{a} \theta \right] = \frac{1}{\rho_0} \frac{\partial p}{\partial x_1},$$

$$- \nu a(f'' + cg'') - a^2(f' + cg')(f + cg) = \frac{1}{\rho_0} \frac{\partial p}{\partial x_2},$$

$$acx_3 \left[\nu g''' + ag''(f + cg) - acg'^2 - \frac{\sigma_e}{\rho} B_0^2 g' \right] = \frac{1}{\rho_0} \frac{\partial p}{\partial x_3}. \tag{17}$$

Then, by integrating $(17)_2$, we find

$$p = -\frac{1}{2}\rho_0 a^2 [f(x_2) + cg(x_2)]^2 - \rho_0 a\nu [f'(x_2) + cg'(x_2)] + P(x_1, x_3),$$

where the function $P(x_1, x_3)$ is determined supposing that, far from the wall, the pressure p has the same behaviour as for an inviscid fluid, whose velocity is given by (8) and the modified pressure is given by (6) replacing x_2 by $x_2 - C$. Therefore, by virtue of (13), and (14), we get

$$P(x_1, x_3) = -\rho_0 \frac{a^2}{2}(x_1{}^2 + c^2 x_3^2) - \frac{a}{2}\sigma_e B_0^2(x_1^2 + cx_3^2) + p_0^*,$$

where p_0^* is a suitable constant. Finally, the modified pressure field assumes the form

$$p = -\rho_0 \frac{a^2}{2}\{x_1^2 + [f(x_2) + cg(x_2)]^2 + c^2 x_3^2\} - \rho_0 a\nu [f'(x_2) + cg'(x_2)]$$
$$- a\sigma_e B_0^2(x_1^2 + cx_3^2) + p_0, \tag{18}$$

where the constant p_0 is the pressure at the origin.
In consideration of (18), we obtain the ordinary differential system

$$\frac{\nu}{a} f''' + (f + cg)f'' - f'^2 + 1 + M^2(1 - f') + \lambda\theta = 0,$$

$$\frac{\nu}{a} g''' + (f + cg)g'' - cg'^2 + c + M^2(1 - g') = 0,$$

$$\beta\theta'' + a(f + cg)\theta' - af'\theta = 0. \tag{19}$$

where

$$M = \sqrt{\frac{\sigma_e B_0^2}{\rho_0 a}}, \qquad \lambda = \frac{g_0 \alpha_T D}{a^2}$$

are the Hartmann number, buoyancy parameter, respectively.
To these equations we append the boundary conditions (12), and (13).
Finally, it is convenient to write the boundary value problem in dimensionless

form in order to reduce the number of the parameters. To this end we put

$$\eta = \sqrt{\frac{a}{\nu}}x_2, \quad \varphi(\eta) = \sqrt{\frac{a}{\nu}}f\left(\sqrt{\frac{\nu}{a}}\eta\right),$$

$$\gamma(\eta) = \sqrt{\frac{a}{\nu}}g\left(\sqrt{\frac{\nu}{a}}\eta\right), \quad \vartheta(\eta) = \theta\left(\sqrt{\frac{\nu}{a}}\eta\right). \tag{20}$$

So we can rewrite equations (19) as:

$$\varphi''' + (\varphi + c\gamma)\varphi'' - \varphi'^2 + 1 + M^2(1 - \varphi') + \lambda\vartheta = 0,$$

$$\gamma''' + (\varphi + c\gamma)\gamma'' - c\gamma'^2 + c + M^2(1 - \gamma') = 0,$$
$$\vartheta'' + Pr(\varphi + c\gamma)\vartheta' - Pr\varphi'\vartheta = 0, \tag{21}$$

where

$$Pr = \frac{\nu}{\beta}$$

is the Prandtl number.
The boundary conditions in dimensionless form become

$$\varphi(0) = 0, \quad \varphi'(0) = 0,$$

$$\gamma(0) = 0, \quad \gamma'(0) = 0, \quad \vartheta(0) = 1$$
$$\lim_{\eta \to +\infty} \varphi'(\eta) = 1, \quad \lim_{\eta \to +\infty} \gamma'(\eta) = 1, \quad \lim_{\eta \to +\infty} \vartheta(\eta) = 0. \tag{22}$$

We underline that the sign of λ is determined by the sign of D, so that we have an assisting or an opposing flow if $\lambda > 0$ or $\lambda < 0$.

The solution of the other two cases of Theorem 2 can be easily obtained with analogous calculations.
Therefore, if we consider

$$\mathbf{H}_0 = H_0\mathbf{e}_1,$$

then the modified pressure field assumes the form

$$p = -\rho_0\frac{a^2}{2}\{x_1^2 + [f(x_2) + cg(x_2)]^2 + c^2x_3^2\} - \rho_0 a\nu[f'(x_2) + cg'(x_2)]$$

$$+ \sigma_e aB_0^2\left\{\int_0^{x_2}[f(s) + cg(s)]ds - \frac{c}{2}x_3^2\right\} + p_0 \tag{23}$$

and the dimensionless functions φ, γ, ϑ satisfy the following equations

$$\varphi''' + (\varphi + c\gamma)\varphi'' - \varphi'^2 + 1 + \lambda\vartheta = 0,$$

$$\gamma''' + (\varphi + c\gamma)\gamma'' - c\gamma'^2 + c + M^2(1 - \gamma') = 0,$$
$$\vartheta'' + Pr(\varphi + c\gamma)\vartheta' - Pr\varphi'\vartheta = 0. \tag{24}$$

8

Finally, if

$$\mathbf{H}_0 = H_0 \mathbf{e}_3.$$

then the modified pressure field assumes the form

$$p = -\rho \frac{a^2}{2} \{ x_1^2 + [f(x_2) + cg(x_2)]^2 + c^2 x_3^2 \} - \rho a \nu [f'(x_2) + cg'(x_2)]$$

$$+ \sigma_e a B_0^2 \left\{ \int_0^{x_2} [f(s) + cg(s)] ds - \frac{1}{2} x_1^2 \right\} + p_0 \tag{25}$$

and the dimensionless functions φ, γ, ϑ satisfy the following equations

$$\varphi''' + (\varphi + c\gamma)\varphi'' - \varphi'^2 + 1 + M^2(1 - \varphi') + \lambda\vartheta = 0,$$

$$\gamma''' + (\varphi + c\gamma)\gamma'' - c\gamma'^2 + c = 0,$$

$$\vartheta'' + Pr(\varphi + c\gamma)\vartheta' - Pr\varphi'\vartheta = 0. \tag{26}$$

Of course to the systems (24), (26) we have to add the boundary conditions (22).

We now analyze the cases considered in Remark 3. Contrary to what happens for the inviscid fluid, we have the following result:

Proposition 6. *Let a homogeneous, incompressible, electrically conducting Newtonian fluid occupy the half-space $\mathcal{S}$. If we neglect the induced magnetic field and we suppose either*

$$i) \quad c = 1, \quad \mathbf{H_0} \text{ parallel to the plane } Ox_1x_3,$$

or

$$ii) \quad c = -\frac{1}{2}, \quad \mathbf{H_0} \text{ parallel to the plane } Ox_2x_3,$$

then there is no solution to problem (9), (11), (12), (13).

Proof. i) Suppose $c = 1$ and the external magnetic induction field given by $\mathbf{B}_0 = B_{01}\mathbf{e}_1 + B_{03}\mathbf{e}_3$ $(B_{01}, B_{03} \neq 0)$. From equations (9), (11), proceeding as previously, after some calculations, we deduce:

$$\varphi''' + (\varphi + \gamma)\varphi'' - \varphi'^2 + 1 + M_3^2(1 - \varphi') + \lambda\vartheta = 0,$$

$$\gamma' - 1 = 0,$$

$$\gamma''' + (\varphi + \gamma)\gamma'' - \gamma'^2 + 1 + M_1^2(1 - \gamma') = 0,$$

$$\varphi' - 1 = 0,$$

$$\vartheta'' + Pr(\varphi + \gamma)\vartheta' - Pr\varphi'\vartheta = 0, \tag{27}$$

where

$$M_1^2 = \frac{\sigma_e B_{01}^2}{\rho_0 a}, \quad M_3^2 = \frac{\sigma_e B_{03}^2}{\rho_0 a}.$$

9

From $(27)_2, (27)_4$ one has $\varphi' = \gamma' = 1$ for all $\eta \geq 0$ which contradicts the boundary conditions $(22)_2$, $(22)_4$.

ii) Now we examine the case $c = -\dfrac{1}{2}$ and $\mathbf{B}_0 = B_{02}\mathbf{e}_2 + B_{03}\mathbf{e}_3$ $(B_{02}, B_{03} \neq 0)$. By proceeding as above, we obtain

$$\varphi''' + (\varphi - \frac{\gamma}{2})\varphi'' - \varphi'^2 + 1 + (M_2^2 + M_3^2)(1 - \varphi') + \lambda\vartheta = 0,$$

$$\gamma''' + (\varphi - \frac{\gamma}{2})\gamma'' + \frac{1}{2}\gamma'^2 - \frac{1}{2} + M_2^2(1 - \gamma') = 0,,$$

$$\varphi - \gamma + A^* - B^* = 0,$$

$$\vartheta'' + Pr(\varphi - \frac{1}{2}\gamma)\vartheta' - Pr\varphi'\vartheta = 0, \tag{28}$$

where

$$M_2^2 = \frac{\sigma_e B_{02}^2}{\rho_0 a}, \quad A^* = \sqrt{\frac{a}{\nu}}A, \quad B^* = \sqrt{\frac{a}{\nu}}B.$$

From $(28)_3$ evaluated at $\eta = 0$ and $(22)_1$ -3, we obtain $\varphi = \gamma$ and $A^* = B^*$, $\forall \eta \geq 0$. So $(28)_1$, $(28)_2$, $(28)_4$ become

$$\varphi''' + \frac{\varphi}{2}\varphi'' - \varphi'^2 + 1 + (M_2^2 + M_3^2)(1 - \varphi') + \lambda\vartheta = 0,$$

$$\varphi''' + \frac{\varphi}{2}\varphi'' + \frac{1}{2}\varphi'^2 - \frac{1}{2} + M_2^2(1 - \varphi') = 0,$$

$$\vartheta'' + Pr(\frac{1}{2}\varphi\vartheta' - \varphi'\vartheta) = 0. \tag{29}$$

By subtracting $(29)_1$ from $(29)_2$, we arrive at

$$\frac{3}{2}(\varphi'^2 - 1) + M_3^2(\varphi' - 1) - \lambda\vartheta = 0. \tag{30}$$

At $\eta = 0$, (30) gives

$$\frac{3}{2} + M_3^2 + \lambda = 0.$$

If $\lambda > 0$ (i.e. $D > 0$), then we get an absurdum and so the thesis is proved. If $\lambda < 0$ (i.e. $D < 0$), then

$$\lambda \equiv \lambda^* = -\left(\frac{3}{2} + M_3^2\right). \tag{31}$$

In order to prove that also for $\lambda = \lambda^*$ the problem does not admit solution, we begin by differentiate twice equation (30):

$$3\varphi'\varphi'' + M_3^2\varphi'' - \lambda^*\vartheta' = 0,$$
$$3(\varphi''^2 + \varphi'\varphi''') + M_3^2\varphi''' - \lambda^*\vartheta'' = 0 \tag{32}$$

10

from which, taking into account $(29)_3$ and the boundary conditions, we deduce

$$\vartheta'(0) = \frac{M_3^2 \varphi''(0)}{\lambda^*}, \quad \varphi''(0)^2 = -\frac{M_3^2}{3} \varphi'''(0). \tag{33}$$

On the other hand equation $(29)_2$ furnishes

$$\varphi'''(0) = \frac{1}{2} - M_2^2 \tag{34}$$

so that from $(33)_2$ follows an absurdum if $M_2^2 < \frac{1}{2}$.

Now we suppose $M_2^2 > \frac{1}{2}$ and we differentiate $(29)_2$, $(29)_3$, $(32)_2$ to arrive at

$$\varphi^{IV}(0) = M_2^2 \varphi''(0), \quad \vartheta'''(0) = Pr \varphi''(0)$$
$$M_2^2(M_3^2 - 9) + \frac{9}{2} - \lambda^* Pr = 0. \tag{35}$$

Moreover, by means of another differentiation of $(29)_2$, $(29)_3$, $(32)_2$, we obtain

$$\varphi^V(0) = -\frac{3}{2} \varphi''^2(0) + M_2^2 \varphi'''(0), \quad \vartheta^{IV}(0) = Pr \left[\varphi'''(0) + \frac{3}{2} \frac{M_3^2 \varphi''^2(0)}{\lambda^*} \right]$$
$$M_3^4(1 + Pr) - M_3^2(9 + Pr) + 12(3 + Pr) = 0. \tag{36}$$

Equation $(36)_3$ does not admit real solutions M_3^2 and so we have a contradiction. Finally, if $M_2^2 = \frac{1}{2}$ then it is easy to verify that φ has equal to zero all derivatives at $\eta = 0$ from which we deduce that $\varphi(\eta) = 0 \quad \forall \eta \geq 0$. This contradicts the boundary condition $(22)_6$. □

Remark 7. *The shear components of the skin friction τ_1 and τ_3 in the x_1 and x_3 directions are:*

$$\tau_1 = \mu \left(\frac{\partial v_1}{\partial x_2} \right)_{x_2=0} = \rho_0 a \sqrt{\nu a} \, x_1 \varphi''(0),$$

$$\tau_3 = \mu \left(\frac{\partial v_3}{\partial x_2} \right)_{x_2=0} = c \rho_0 a \sqrt{\nu a} \, x_3 \gamma''(0). \tag{37}$$

From the practical point of view, it is interesting to compute the heat flux in the x_2-direction at $x_2 = 0$:

$$q_w = -k \frac{\partial T}{\partial x_2} \Big|_{x_2=0} = -k D x_1 \sqrt{\frac{a}{\nu}} \vartheta'(0),$$

where k is the fluid thermal conductivity.

Remark 8. *In the absence of the external magnetic field and of buoyancy forces for the three-dimensional stagnation-point flow, the numerical results*

([21], [22]) show that there exists a negative value of c (c_r) such that if $c \geq c_r$, then $\gamma', \gamma'' > 0 \ \forall \eta > 0$, and if $c < c_r$ then near the wall $\gamma', \gamma'' < 0$, so that the reverse flow appears because the v_3 component of the velocity reverses its direction. The reverse flow is also related to a sign change of τ_3. This phenomenon has been found also in the presence of a uniform external magnetic field in isothermal conditions [3].

As we will see in Section 4, in our problem by virtue of buoyancy forces this phenomenon appears not only for v_3 but also for v_1 if λ takes particular negative values. In this case also τ_1 presents a sign change. The presence of the external magnetic field tends to prevent the occurrence of the reverse flow while the buoyancy forces tend to favor it. This behaviour has been observed in several other physical situations [4], [5], [13].

Remark 9. As it is underlined in [32], at a very small distance η from the surface of an obstacle, the velocity of a Newtonian fluid is approximately

$$\mathbf{v} \cong \sqrt{\frac{\nu}{a}} \frac{\tau_0}{\mu} \eta, \tag{38}$$

where τ_0 is the skin friction vector, which in our situation is given by

$$\tau_0 = \rho_0 a \sqrt{\nu a}[x_1 \varphi''(0)\mathbf{e}_1 + c x_3 \gamma''(0)\mathbf{e}_3]. \tag{39}$$

Moreover the normal component of the velocity at a higher order of approximation is

$$v_2 \cong -\frac{1}{2}\frac{\nu}{a} div\left(\frac{\tau_0}{\mu}\right)\eta^2 := -\frac{1}{2}\Delta_s \eta^2. \tag{40}$$

We see from (38) that close to the obstacle the direction of streamlines becomes parallel to its surface, except where $\tau_0 = \mathbf{0}$. This condition that both tangential components of skin friction vanish simultaneously, is satisfied in general only at isolated points of the surface, which are called 'points of separation' if $\Delta_s < 0$ (so that the normal velocity (40) is positive) and 'points of attachment' if $\Delta_s > 0$. In our analysis, the only isolated point such that $\tau_0 = \mathbf{0}$ is the origin, i.e. the stagnation-point, and

$$\Delta_s = \sqrt{\nu a}[\varphi''(0) + c\gamma''(0)].$$

Streamlines very near to the surface lie closely along the skin friction line, as (38) indicates.

There is just one skin friction line and one vortex line through each point of the surface, except a point of attachment or separation. These last are 'singular points' of the differential equations of both systems of curves. Such singular points are classified into two main types, depending on the sign of:

$$J_s = \frac{\partial \tau_{01}}{\partial x_1}\frac{\partial \tau_{03}}{\partial x_3} - \frac{\partial \tau_{01}}{\partial x_3}\frac{\partial \tau_{03}}{\partial x_1}. \tag{41}$$

A singular point where $J_s < 0$ is a 'saddle point', and where $J_s > 0$ there is a 'nodal point'.
We remark that we have

$$J_s = \rho_0{}^2 \nu a^3 [c\varphi''(0)\gamma''(0)].$$

From these considerations it is clear that we need to know the signs of $c, \varphi''(0), \gamma''(0)$ in order to classify the stagnation-point.
As it is underlined in [22], in the case $M = 0$, $\lambda = 0$ and $Pr = 0$ from the numerical results one has that the stagnation-point is a nodal point of attachment if $c > 0$ or $c < c_r = -0.4294$, while it is a saddle point of attachment if $c_r \le c < 0$. We remark that in [22] the Author corrected the classification of the stagnation-point contained in [21]. In the literature, most of the papers refer to the uncorrected classification in [21].

4. Numerical results and discussion

In this section we furnish the numerical solution only for problem (21), (22) because it is the most relevant from a physical point of view.
The system of ordinary differential equations (21) subject to the boundary conditions (22) was solved numerically using the function bvp4c from MATLAB for different values of the Hartmann number M, buoyancy parameter λ and constant c when the Prandtl number is fixed $Pr = 0.71$. The parameter c is a measure of the three-dimensionality of the motion because when $c = 0$ the problem reduces to the case of the plane orthogonal stagnation-point flow.
The routine bvp4c is a finite difference code that implements the three-stage Lobatto IIIa formula, which is a collocation formula with forth-order accuracy. The mesh selection and error control are based on the residual of the continuous solution. We set here the relative error tolerance to 10^{-7}. Since the present boundary value problem may have more than one (dual) solution, upper and lower branch solutions, a 'good' initial guess is necessary to obtain the desired solutions of Eqs. (21) with boundary conditions (22). The guess should satisfy the boundary conditions (22) and show the correct asymptotic behavior of the solution. Determining an initial guess for the first (upper branch) solution is not difficult because the bvp4c method will converge to the first solution even for very poor guesses. However, the hardest part is to come up with a sufficiently good guess for the solution of the system of the ordinary differential Eqs. (21) in the case of opposing flow when $\lambda < 0$. To overcome this difficulty, we start with a set of parameter values determined by trials for which the problem is easy to be solved and for which the second solution is obtained. Then, we use the obtained solution as initial guess for other solutions of the problem with small variation of the desired parameters. This is repeated until we obtain the right values of the parameters we are interested in. The 'infinity' in the boundary conditions (21) is replaced with a finite number. In practice, we start the computation at a small value, for example $\eta = 10$, then subsequently increase the value of η until we obtain the convergence at sufficiently 'large' boundary

Table 1: Comparison of $\varphi''(0)$ for several values of Pr when $M = c = 0$ and $\lambda = 1$.

Pr	Ramachandran et al. [19]	Ishak et al. [20]		Present study	
	first solution	first solution	second solution	first solution	second solution
0.7	1.7063	1.7063	1.2387	1.7063	1.2387
1	-	1.6754	1.1332	1.6754	1.1332
7	1.5179	1.5179	0.5824	1.5179	0.5824
10	-	1.4928	0.4958	1.4928	0.4958
20	1.4485	1.4485	0.3436	1.4485	0.3436
40	1.4101	1.4101	0.2111	1.4101	0.2111
50	-	1.3989	0.1720	1.3989	0.1720
60	1.3903	1.3903	0.1413	1.3903	0.1413
80	1.3774	1.3774	0.0947	1.3774	0.0947
100	1.3680	1.3680	0.0601	1.3680	0.0601

layer thickness $\eta = \eta_\infty$. In this method, we have chosen a suitable finite value of η_∞, namely $\eta = \eta_\infty = 20$ for the upper branch solution and $\eta = \eta_\infty$ in the range $40 - 120$ for the lower branch solution. The converged solution is identified when the plot of $\varphi'(\eta)$ approaches 1, $\gamma'(\eta)$ approaches 1 and $\vartheta(\eta)$ approaches 0 asymptotically with the maximum residuals less than 10^{-7}. This technique is called 'continuation' and is described quite well in the book by Shampine et al. ([17]) or through online tutorial by Shampine and Kierzenka ([18]). This method can be successfully used to solve various problems related to boundary layer flow and heat transfer. The values of the reduced shear components of the skin friction $\varphi''(0)$ and the values of the reduced heat flux from the surface $-\vartheta'(0)$ are obtained and compared with previously reported results by Ramachandran et al. ([19]) and Ishak et al. ([20]) in Tables 1 and 2 when $M = c = 0$ and $\lambda = 1$ (assisting flow) for several values of Pr. It is seen that the comparison is in very good agreement, and thus gives us confidence to the accuracy of the numerical results presented in this paper.

The reduced skin friction coefficients $\varphi''(0), \gamma''(0)$, and reduced heat flux $-\vartheta'(0)$ are presented in Figs. 2 to 7.

It is seen from these figures that multiple (dual) solutions of the boundary value problem (21), (22) exist, first (upper branch) and second (lower branch) solutions for some values of the parameters M and c for negative (opposing flow) values of the mixed convection parameter λ with fixed value of $Pr = 0.71$. There are two solutions when $\lambda > \lambda_c$ in a certain range of $\lambda < 0$, one solution when $\lambda = \lambda_c$ and no solution when $\lambda < \lambda_c$, where $\lambda_c < 0$ is the critical value of λ for which the solution exists. It should be mentioned that for $\lambda < \lambda_c$ the ordinary differential equations (21) subject to the boundary conditions (22) have no solutions. Further, it should be mentioned that the existence of the

Table 2: Comparison of $-\vartheta'(0)$ for several values of Pr when $M = c = 0$ and $\lambda = 1$.

| Pr	Ramachandran et al.	Ishak et al.		Present study	
	first solution	first solution	second solution	first solution	second solution
0.7	0.7641	0.7641	1.0226	0.7641	1.0226
1	-	0.8708	1.1691	0.8708	1.1691
7	1.7224	1.7224	2.2192	1.7224	2.2192
10	-	1.9446	2.4940	1.9446	2.4940
20	2.4576	2.4576	3.1646	2.4576	3.1646
40	3.1011	3.1011	4.1080	3.1011	4.1080
50	-	3.3415	4.4976	3.3415	4.4976
60	3.5514	3.5514	4.8572	3.5514	4.8572
80	3.9095	3.9095	5.5166	3.9095	5.5166
100	4.2116	4.2116	6.1230	4.2116	6.1230
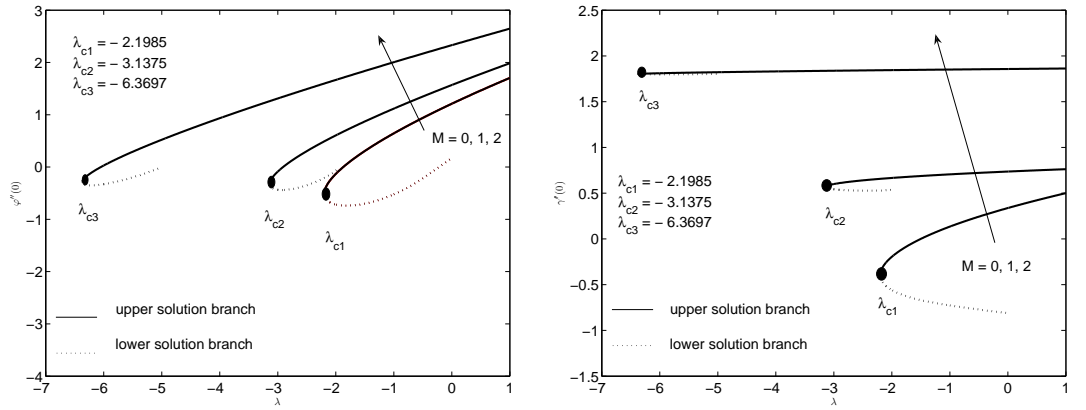
Figure 2: Plots showing variation of $\varphi''(0)$ and $\gamma''(0)$ with λ for several values of $M = 0, 1, 2$ when $c = -0.5$ and $Pr = 0.71$, respectively.
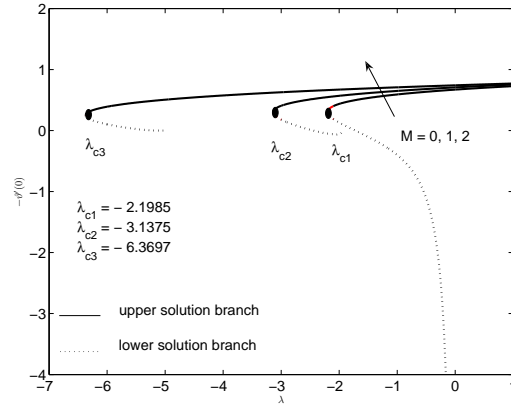
Figure 3: Plots showing variation of $-\vartheta'(0)$ with λ for several values of $M = 0, 1, 2$ when $c = -0.5$ and $Pr = 0.71$.
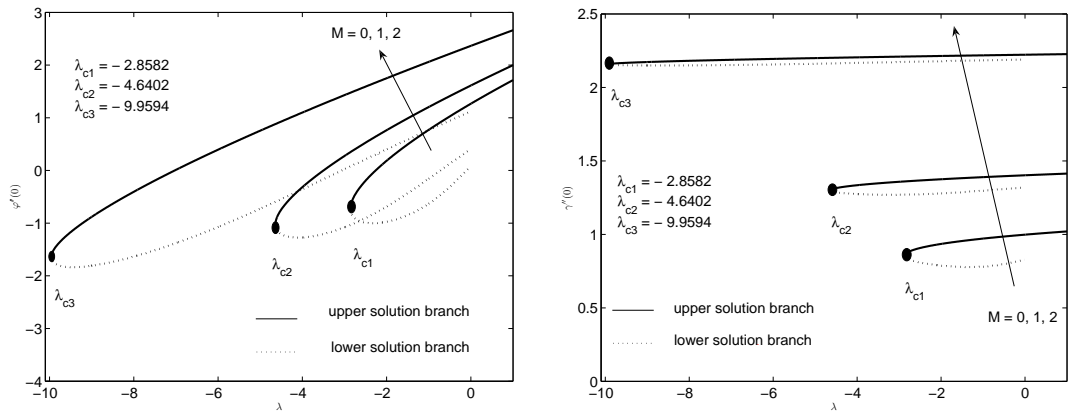

Figure 4: Plots showing variation of $\varphi''(0)$ and $\gamma''(0)$ with λ for several values of $M = 0, 1, 2$ when $c = 0.5$ and $Pr = 0.71$, respectively.
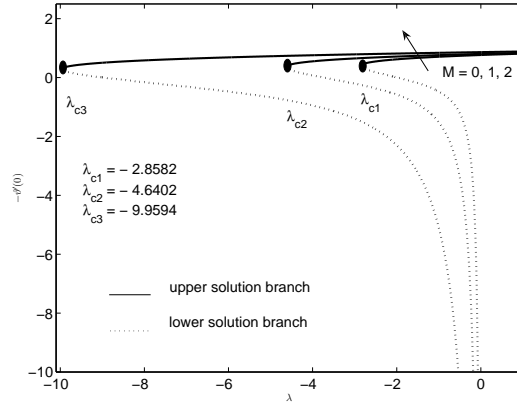
16

Figure 5: Plots showing variation of $-\vartheta'(0)$ with λ for several values of $M = 0, 1, 2$ when $c = 0.5$ and $Pr = 0.71$.
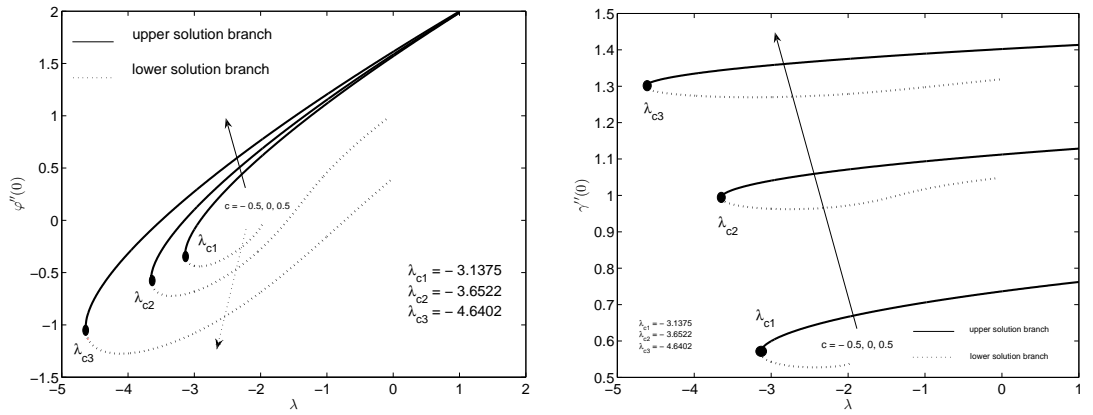

Figure 6: Plots showing variation of $\varphi''(0)$ and $\gamma''(0)$ with λ for several values of $c = -0.5, 0, 0.5$ when $M = 1$ and $Pr = 0.71$, respectively.
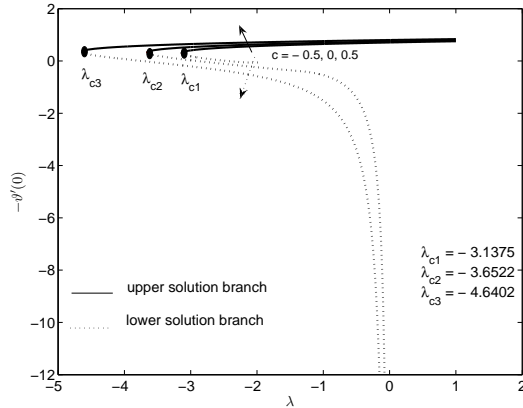
Figure 7: Plots showing variation of $-\vartheta'(0)$ with λ for several values of $c = -0.5, 0, 0.5$ when $M = 1$ and $Pr = 0.71$.

multiple solutions results in from a linear stability analysis. However, we do not present such an analysis in this paper. From the stability analysis one can see that the upper branch solutions are stable and, thus, physically realizable, while the lower branch solutions are unstable and, therefore, not physically realizable. These lower branch solutions appear only from numerical reasons. The existence of dual solutions for the similar problems was also reported by Weidman et al. ([23]), Ishak et al. ([24, 20, 8, 14]), Bhattacharyya ([25]), Bhattacharyya and Vajravelu ([26]), Bachok et al. ([27, 28, 29]) and Roşca and Pop ([30, 31]) among others. One can see from Figs. 2 to 5 that for both positive and negative values of c, as the Hartmann number parameter M increases, the magnitude of the absolute critical value $|\lambda_c|$ increases as well. This suggest that the magnetic effect is to widen the range of λ for which the solution to the system of equations (21) with the boundary conditions (22) exists. The effect of the parameter c on the reduced skin friction coefficients $\varphi''(0), \gamma''(0)$ and reduced heat flux from the wall $-\vartheta'(0)$ is similar, when M is fixed, as can be seen from Figs. 6 and 7. The effects of the parameter λ when M, c and Pr are fixed on the profiles $\varphi'(\eta)$, $\gamma'(\eta)$ and $\vartheta'(\eta)$ are presented in Figs. 8 and 9.

The far field boundary conditions (22) are satisfied asymptotically, which supports the validity of the numerical results obtained.
Further, it is observed from the profiles presented in these figures that there are two (upper and lower) profiles for a particular value of the parameter $\lambda < 0$ (opposing flow), while the other parameters are fixed. The number of solutions depends on the range of the parameter λ. Moreover, we notice from these figures that for all profiles, the first solutions display a thinner boundary layer thickness compared to the second solutions.
Finally me examine the phenomenon of the reverse flow and the classification
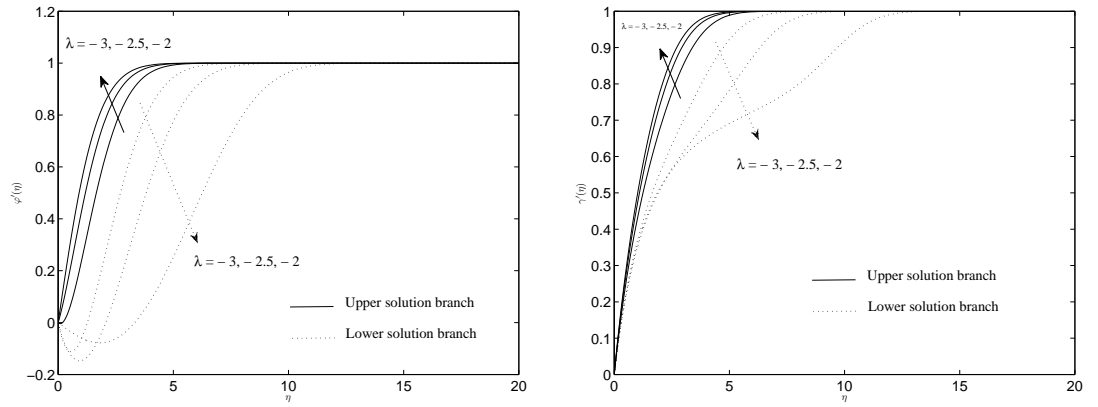
18

Figure 8: Profiles showing $\varphi'(\eta)$ and $\gamma'(\eta)$ for several values of λ when $c = -0.5$, $M = 1$ and $Pr = 0.71$, respectively.
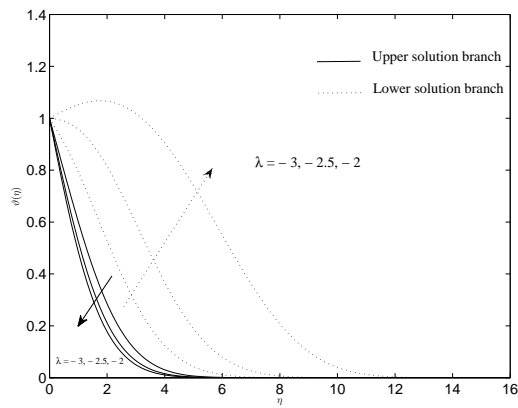

Figure 9: Profiles showing $\vartheta(\eta)$ for several values of λ when $c = -0.5$, $M = 1$ and $Pr = 0.71$.

of the stagnation point.

Figure 2_1 shows that the reverse flow occurs for v_1 for suitable negative values of λ also for the lower solution branch. As far as v_3 is concerned figure 2_2 indicates that the reverse flow appears only for $M = 0$ and $\lambda < 0$. We see that the presence of the external uniform magnetic filed tends to prevent the reversal of motion. Figures 4_1, 6_1 confirm the phenomenon also for $c > 0$ while figures 4_2, 6_2 show that the reverse flow does not occur for v_3 for the values of the parameters considered.

The figures relative to temperature show that $-\vartheta'(0)$ is positive for the upper solution while can take negative values for the lower solution. Moreover they suggest that reduced heat flux at the wall for the lower branch solution becomes unbounded as $\lambda \to 0^-$ and as $\lambda \to 0^+$.

Table 3 illustrates the influence of M, λ on c_r and so on the behavior of v_3. For $M, \lambda = 0$ we find the critical value of c furnished in [22]. When $M = 0$, the reverse flow for v_3 occurs also for positive values of λ and we see that c_r decreases as λ increases. When $\lambda < 0$ (opposite flow) the critical value of c is greater than that one given in [22] and so the reverse flow is favored. When $M = 1, 2$ only sufficiently small negative values of λ determine this phenomenon while in the absence of the buoyancy forces the reverse flow does not occur when $M^2 \geq 0.7583$ ([3]). We note that the trend of c_r is the same as for $M = 0$. Therefore we can conclude that the external magnetic field tends to prevent the reverse flow for v_3 while the buoyancy forces tend to favor it.

Finally in table 4 we present $\varphi''(0)$ and $\gamma''(0)$ for first and second solution for different values of the parameters M, λ and c when $Pr = 0.71$ in order to classify the origin. We find when the origin is a nodal point of attachment (n.a.) or of separation (n.s.) and when it is a saddle point of attachment (s.a.) or of separation (s.s.) We see that there is no difference between upper and lower solution. For $\lambda = 0$ the results are in very good agreement with [3]. Moreover the table 4 confirms the occurrence of reverse flow for v_1 and v_3.

5. Conclusions

A theoretical and numerical study has been performed on the problem of the magnetohydrodynamic mixed convection stagnation-point flow and heat transfer on a vertical flat plate. The effects of the governing parameters on the reduced skin friction coefficient and reduced heat flux from the plate have been analyzed and graphically presented. From this study, the following conclusions could be drawn:

- Dual solutions exist for a certain range of the buoyancy parameter λ.

- Hartmann number M increases the range of the buoyancy parameter for which the solutions exist.

- Reverse flow phenomenon appears for v_1 and v_3 for suitable values of the parameters.

Table 3: Influence of M and λ on the value of c_r an so on v_3.

M	λ	c_r
0	-2.1	-0.2259
	-2	-0.2529
	-1	-0.3655
	0	-0.4294 (as in [22])
	2	-0.5201
	3	-0.5564
	5	-0.6186
1	-3.1	-0.0760
	-3	-0.2511
	-2.95	-0.3601
	-2.91	-0.6785
2	-6.2	-0.3658
	-6	-0.5411
	-5.8	-0.6986
	-5.6	-0.8402

- The external magnetic field tends to prevent the reverse flow.

- The buoyancy forces tend to favor the reverse flow.

References

[1] P.D. Ariel. Hiemenz flow in hydromagnetics. Acta Mech 1994; 103:31-43.

[2] A. Borrelli, G. Giantesio, M.C. Patria. Three-dimensional MHD stagnation point-flow of a Newtonian and a micropolar fluid. IJPAM 2011; 73:165-188.

[3] A. Borrelli, G. Giantesio, M.C. Patria. On the numerical solutions of three-dimensional MHD stagnation point-flow of a Newtonian fluid. IJPAM 2013; 86:425-442.

[4] A. Borrelli, G. Giantesio, M.C. Patria. Effect on a non-uniform magnetic field on the 3D stagnation point-flow. European Journal of Mechanics B/Fluids 2014; 48:210-217.

[5] S. Bhattacharyya, A.S. Gupta. MHD flow and heat transfer at a general three-dimensional stagnation point. Int J of Non-Linear Mech 1998; 33:125-134.

[6] T.R. Mahapatra, S.K. Nandy, A.S. Gupta. Analytical solution of magnetohydrodynamic stagnation-point flow of a power-low fluid towards a stretching surface. Appl Math Comput 2009; 215:1696-1710.

Table 4: Calculated numbers of $\varphi''(0)$ and $\gamma''(0)$ for first and second solution for different values of the parameters M, λ and c when $Pr = 0.71$.

M	λ	c	Upper solution (first solution) $\varphi''(0)$	branch $\gamma''(0)$	stagnation point	Lower solution (second solution) $\varphi''(0)$	branch $\gamma''(0)$
0	-2	-0.5	-0.1315	-0.1951	s.s.	-0.7170	-0.5598
		0.5	0.1839	0.9349	n.a.	-0.9734	0.7874
	-1	-0.6	0.6685	-0.1297	n.a.	-0.6157	-0.8230
		-0.5	0.6438	0.1346	s.a.	-	-
		0.5	0.7709	0.9713	n.a.	-0.6308	0.7807
	0	-0.5	1.2301	-0.1115	n.a.	-	-
		0.5	1.2668	0.9981	n.a.	-	-
	2	-0.6	2.1461	-0.1252	n.a.	-	-
		-0.5	2.1458	0.0309	s.a.	-	-
		-0.3	2.1435	0.3144	s.a.	-	-
		0.5	2.1316	1.0391	n.a.	-	-
1	-3	-0.5	-0.0871	0.5996	n.s.	-0.4359	0.5427
		0.5	0.2745	1.3578	n.a.	-1.0793	1.2700
	-1	-0.5	1.1170	0.7057	s.a.	-	-
		0.5	1.2040	1.3895	n.a.	-0.1553	1.2974
	0	-0.5	1.5687	0.7363	s.a.	-	-
		0.5	1.6125	1.4021	n.a.	-	-
	-0.5	-0.5	1.3483	0.7218	s.a.	-	-
		0.5	1.4115	1.3960	n.a.	0.1292	1.3084
	2	-0.5	2.3766	0.7847	s.a.	-	-
		0.5	2.3667	1.4240	n.a.	-	-
2	-6.2	-0.5	-0.0997	1.8075	n.s.	-0.3513	1.7989
		0.5	0.3195	2.1927	n.a.	-1.1379	2.1553
	-5.5	-0.5	0.2925	1.8170	s.s.	-0.1977	1.7999
		0.5	0.5767	2.1967	n.a.	-0.9040	2.1586
	-2	-0.5	1.6659	1.8448	s.a.	-	-
		0.5	1.7500	2.2139	n.a.	0.4003	2.1785
	-1	-0.5	2.0046	1.8511	s.a.	-	-
		0.5	2.0613	2.2182	n.a.	0.7667	2.1841
	0	-0.5	2.3307	1.8570	s.a.	-	-
		0.5	2.3649	2.2224	n.a.	-	-
	2	-0.5	2.9540	1.8678	s.a.	-	-
		0.5	2.9525	2.2303	n.a.	-	-

[7] T. Grosan, I. Pop, C. Revnic, D.B. Ingham. Magnetohydrodynamic oblique stagnation-point flow. Meccanica 2009;44:565-572.

[8] A. Ishak, R. Nazar, I. Pop. Magnetohydrodynamic stagnation-point flow towards a stretching vertical sheet. Magnetohydrodynamics 2006; 42:17-30.

[9] A. Borrelli, G. Giantesio, M.C. Patria. MHD oblique stagnation-point flow of a Newtonian fluid. ZAMP 2012; 63:271-294.

[10] A. Borrelli, G. Giantesio, M.C. Patria. An exact solution for the 3D MHD stagnation-point flow of a micropolar fluid. CNSNS 2015; 20:121-135.

[11] Y.Y. Lok, A. Ishak, I. Pop. MHD stagnation-point flow towards a shrinking sheet. Int J Numer Methods Heat Fluid Flow 2011; 21:61-72.

[12] H. Xu H, S.J. Liao, I. Pop. Series solutions of unsteady three dimensional MHD flow and heat transfer in a boundary layer over an impulsively streatching plate. Eur J Mech B Fluids 2007; 26:15-27.

[13] A. Borrelli, G. Giantesio, M.C. Patria. Magnetoconvection of a micropolar fluid in a vertical channel. Int J Heat and Mass Transfer 2015; 80:614-625.

[14] I. Pop, A. Ishak, F. Aman. Radiation effects on the MHD flow near the stagnation-point of a stretching sheet: revisited. ZAMP 2011; 62:953-956.

[15] F.M. Ali, R. Nazar, N.M. Arifin, I. Pop. MHD mixed convection boundary layer flow towards a stagnation point on a vertical surface with induced magnetic field. ASME Journal of Heat Transfer 2011; 133:022502-1-022502-6.

[16] F.M. Ali, R. Nazar, N.M. Arifin, I. Pop. MHD stagnation-point flow and heat transfer towards a stretching sheet with induced magnetic field. Appl Math Mech 2011; 32:409-418.

[17] L.F. Shampine, I. Gladwell, S. Thompson. Solving ODEs with Matlab. Cambridge University Press: Cambridge; 2003.

[18] L.F. Shampine, M.W. Reichelt, J. Kierzenka. Solving boundary value problems for ordinary differential equations in MATLAB with bvp4c. http://www.mathworks.com/bvptutorial.

[19] N. Ramachandran, T.S. Chen, B.F. Armaly. Mixed convection in stagnation flows adjacent to a vertical surfaces. ASME J Heat Transfer 1988; 110:373-377.

[20] A. Ishak, R. Nazar, N.M. Arifin, I. Pop. Dual solutions in mixed convection flow near a stagnation point on a vertical porous plate. Int J Thermal Sci 2008; 47:417-422.

[21] A. Davey. Boundary layer flow at a saddle point of attachment. Journal of Fluid Mechanics 1961; 10:593-610.

[22] A. Davey. Rotational flow near a forward stagnation point. The Quarterly Journal of Mechanics and Applied Mathematics 1963; 26:33-59.

[23] P.D. Weidman, D.G. Kubitschek, A.M.J. Davis. The effect of transpiration on self-similar boundary layer flow over moving surfaces. Int J Eng Sci 2006; 44:730-737.

[24] A. Ishak, R. Nazar, N.M. Arifin, I. Pop. Dual solutions in magnetohydrodynamic mixed convection flow near a stagnation-point on a vertical surface. ASME J Heat Transfer 2007; 129:1212-125.

[25] K. Bhattacharyya. Boundary layer flow and heat transfer over an exponentially shrinking sheet. Chin Phys Lett 2011; 28:074701.

[26] K. Bhattacharyya, K. Vajravelu. Stagnation-point flow and heat transfer over an exponentially shrinking sheet. CNSNS 2012; 17:2728-2734.

[27] N. Bachok, A. Ishak, I. Pop. Unsteady boundary-layer flow and heat transfer of a nanofluid over a permeable stretching/shrinking sheet. Int J Heat Mass Transfer 2012; 55:2102-2109.

[28] N. Bachok, A. Ishak, I. Pop. The boundary layers of an unsteady stagnation-point flow in a nanofluid. Int J Heat Mass Transfer 2012; 55:6499-6505.

[29] N. Bachok, A. Ishak, I. Pop. Boundary layer stagnation-point flow toward a stretching/shrinking sheet in a nanofluid. ASME J Heat Transfer 2013; 135:054501.

[30] N.C. Roşca, I. Pop. Mixed convection stagnation point flow past a vertical flat plate with a second order slip: heat flux case. Int J Heat Mass Transfer 2013; 65:102-109.

[31] A.V. Roşca, I. Pop. Flow and heat transfer over a vertical permeable stretching/shrinking sheet with a second order slip. Int J Heat Mass Transfer 2013; 60:355-364.

[32] M. J. Lighthill. Laminar boundary layers. ed. L. Rosenhead, Dover Publ: Oxford; 1963.